JOURNAL OF VIROLOGY, Oct. 2000, p. 9256–9266 Vol. 74, No. 19
0022-538X/00/$04.00+0

Distinct Trafficking Pathways Mediate Nef-Induced and Clathrin-Dependent Major Histocompatibility Complex Class I Down-Regulation

SYLVIE LE GALL,[1] FLORENCE BUSEYNE,[2] ALICJA TROCHA,[3] BRUCE D. WALKER,[3] JEAN-MICHEL HEARD,[1] AND OLIVIER SCHWARTZ[1]*

Unité Rétrovirus et Transfert Génétique, URA CNRS 1930,[1] and Laboratoire d'Immunopathologie Virale,[2] Institut Pasteur, 75724 Paris Cedex 15, France, and Partners AIDS Research Center, Massachusetts General Hospital, Charlestown, Massachusetts 02129[3]

Received 22 February 2000/Accepted 11 July 2000

The human immunodeficiency virus type 1 Nef protein alters the post-Golgi stages of major histocompatibility complex class I (MHC-I) biogenesis. Presumed mechanisms involve the disclosure of a cryptic tyrosine-based sorting signal (YSQA) located in the cytoplasmic tail of HLA-A and -B heavy chains. We changed this signal for a prototypic sorting motif (YSQI or YSQL). Modified HLA-A2 molecules, termed A2-endo, displayed constitutively low surface levels and accumulated in a region close to or within the Golgi apparatus, a behavior reminiscent of wild-type HLA-A2 in Nef-expressing cells. However, several lines of evidence indicate that the action of prototypic signals on MHC-I trafficking differs from that of Nef. Internalization of surface A2-endo was more rapid and was associated with efficient recycling to the surface. A transdominant-negative mutant of dynamin-1 inhibited A2-endo constitutive internalization and Nef-induced CD4 down-regulation, whereas it did not affect the activity of Nef on MHC-I. Moreover, trafficking of A2-endo was still affected by the viral protein, indicating additive effects of prototypic signals and Nef. Therefore, distinct trafficking pathways regulate clathrin-dependent and Nef-induced MHC-I modulation.

Major histocompatibility complex class I (MHC-I) molecules present cellular and pathogen-derived peptides to antigen-specific receptors on CD8 T cells. The initial steps of MHC-I biosynthetic and transport pathways are well characterized. Proteolysis of intracellular proteins generates peptides, which are actively transported into the endoplasmic reticulum (ER) for assembly with MHC-I (36, 50). Key actors include the multicatalytic proteasome; ER chaperones (calnexin and calreticulin); TAPs (transporters associated with antigen processing), which translocate peptides across the ER membrane; and tapasin, a protein which bridges MHC-I and TAPs. MHC-I trimolecular complexes, which consist of a highly polymorphic heavy chain, β2-microglobulin, and the antigenic peptide, are then routed through the Golgi to the cell surface.

Post-Golgi trafficking steps are less understood. Although MHC-I molecules are stably expressed at the plasma membrane, a fraction is spontaneously internalized and recycled in T cells and in monocytes/macrophages (25, 38). The biological role of MHC-I recycling is not fully understood, but includes the optimization of peptide loading (1, 19). MHC-I internalization is accelerated by anti-MHC-I antibodies or during T-cell activation (25, 38, 46). In contrast, MHC-I endocytosis is barely observed in fibroblasts (25, 38). Internalized molecules are detected in early endosomes located close to or within the Golgi and are either recycled to the cell surface or end up being degraded (8, 19, 50). They may also enter classical MHC-II compartments (8, 19). MHC-I recycling occurs through clathrin-coated pits and involves determinants borne by the heavy chain cytoplasmic tail (13, 23, 46). However, none of the so-far-identified prototypic sorting signals mediating clathrin-dependent endocytosis are found in this region (21).

Prototypic sorting signals direct transmembrane proteins to various intracellular compartments, including the *trans*-Golgi network (TGN), endosomes, and lysosomes. Sorting signals are located in the cytoplasmic tail of proteins to be sorted and are recognized by adaptor protein (AP) complexes (5). AP complexes are involved in the formation of transport intermediates, such as clathrin-coated pits and clathrin-coated vesicles (CCVs). Four related AP complexes have been described so far: AP-1 and AP-2 target TGN and plasma membrane proteins, respectively, to endosomes (5); AP-3 participates in transport from the Golgi to lysosomes (43); AP-4 is localized at the TGN or a neighboring compartment (14). Sorting motifs located in cytoplasmic domains mostly consist of a leucine-based or tyrosine-based motif (LΦ and YXXΦ, respectively, where X represents any residue and Φ is an amino acid with a bulky hydrophobic chain, such as L or I). The medium (μ) chain of AP complexes binds tyrosine-based motifs (26, 28). The ligand of leucine-based signals may be the μ or β chains of AP-1 and AP-2 (6, 37).

In human immunodeficiency virus (HIV)-infected cells, MHC-I cell surface expression is down-regulated due to the action of the viral protein Nef (42). Synthesis and transport through the ER and *cis*-Golgi occurs normally, but MHC-I molecules from both the Golgi and the cell surface are misrouted towards the endosomal pathway (21, 42). MHC-I molecules accumulate in a perinuclear region which also contains proteins known to be abundant in the TGN (rab6 and γ-adaptin), as well as in more peripheral vesicles positive for endosomal markers (transferrin and clathrin). MHC-I molecules end up being degraded in lysosomes (42). Nef-responsive determinants are contained within the cytoplasmic tail of MHC-I (21). Tyrosine 321 (21), which is conserved in HLA-A and -B, and not in HLA-C and -E molecules, and two other

* Corresponding author. Mailing address: Unité Rétrovirus et Transfert Génétique, URA CNRS 1930, Institut Pasteur, 28 rue du Dr. Roux, 75724 Paris Cedex 15, France. Phone: 33 1 45 68 83 53. Fax: 33 1 45 68 89 40. E-mail: schwartz@pasteur.fr.

residues (alanine 325 and aspartic acid 328) (9) lying within 7 amino acids (aa) of each other are necessary for Nef activity. Cohen et al. observed that these three residues would lie on the same face if they were displayed as an alpha helix, suggesting a potential interaction surface on the cytoplasmic tail of MHC-I molecules (9). With respect to the protective effect of HLA-C and -E against lysis by natural killer (NK) cells, the selective modulation of HLA-A and -B by Nef (21) allows HIV-infected cells to escape from both virus-specific cytotoxic T lymphocytes (CTLs) and NK cells (9, 10).

Tyrosine 321 of MHC-I may be considered as part of a degenerated YXXΦ motif (YSQA). Since an interaction between Nef and the μ chain of AP complexes was revealed by the yeast two-hybrid system and in vitro with recombinant proteins (21, 32), a model was proposed in which Nef would disclose an otherwise cryptic signal (YSQA) to the AP-dependent sorting machinery. The validity of this model was supported by the resemblance of the effects of Nef on MHC-I and CD4. Indeed, Nef acts as a connector between CD4 and the clathrin-dependent sorting machinery (27, 34), and Nef mutants unable to bind AP complexes neither colocalize with clathrin nor down-regulate CD4 (7, 11, 17, 24, 39). However, by comparing Nef mutants for their ability to affect either CD4 or MHC-I expression, it was determined that Nef-induced CD4 down-regulation and MHC-I down-regulation constitute genetically and functionally separate properties (17, 24, 39). In particular, Nef mutants unable to bind AP complexes still modulate MHC-I, suggesting that this interaction may be not required for MHC-I down-regulation.

Here, we investigated this issue further by designing HLA-A2 molecules, termed A2-endo, which carry prototypic sorting signals (YSQI or YSQL) instead of the degenerated motif YSQA. We compared the spontaneous trafficking of A2-endo to that of wild-type (WT) HLA-A2 in the presence of Nef. A2-endo surface expression was constitutively reduced; molecules showed rapid internalization, recycling, and retention in a perinuclear region likely corresponding to the Golgi. However, we demonstrate that distinct trafficking pathways regulate clathrin-dependent and Nef-induced MHC-I modulation. We also show that the steady-state surface level of MHC-I, which can be modulated by rapid endocytosis or by the viral protein Nef, influences MHC-I-restricted lysis of target cells.

MATERIALS AND METHODS

Plasmid construction. The A2 WT vector, containing the HLA-A2 gene downstream of the cytomegalovirus promoter in pcDNA3 (Invitrogen), was described previously (21). HLA-A2 mutants were generated by PCR and inserted into pcDNA3. The sequence of HLA-A2 mutants was verified by sequencing. The Nef-FT, and Nef-mock vectors carrying the *Nef LAI* gene in a sense and antisense orientation, respectively, were described previously (21). The green fluorescent protein (GFP) vector (pEGFP) was obtained from Clontech. Dynamin-1 WT and K44A cDNAs were a gift from S. Schmid (University of California, San Diego) (12) and were subcloned in pcDNA3, yielding dynamin-1 WT and dynamin-1 K44A vectors, respectively. The HIV strain used is the BRU-HA infectious clone, and it contains a hemagglutinin (HA)-tagged integrase (31). BRU-HAΔNef was constructed by inserting a frameshift mutation at the unique *Xho*I site of the provirus. The CD4 vector pCCD4 was obtained by inserting the CD4 cDNA in pcDNA3.

Cell analysis and reagents. Electroporation of HeLa cells, flow cytometry, and indirect immunofluorescence staining were performed as described previously (21). Anti-HLA-A2 monoclonal antibodies (MAbs) BB7.2 and MA2.1 provided by F. Lemonnier (Institut Pasteur) were used (42). An anti-transferrin receptor phycoerythrin (PE)-conjugated MAb (anti-CD71 PE) was obtained from Immunotech. Wheat germ agglutinin (WGA) conjugated to Alexa 488 was obtained from Molecular Probes. Nocodazole was obtained from Sigma. Secondary antibodies were obtained from Southern Biotechnologies.

FACS-based internalization assay. The fluorescence-activated cell sorter (FACS)-based internalization assay was performed as follows. HeLa cells were transiently transfected with the indicated HLA-A2 vectors, along with a GFP vector to distinguish the fraction of transfected cells. After 24 h, cells were incubated at 4°C with the MA2.1 anti-HLA-A2 MAb in phosphate-buffered saline (PBS)–1% bovine serum albumin, washed, and incubated at 37°C in culture medium (containing 20 mM HEPES [pH 7.4]). At different periods of time, MA2.1-bound HLA-A2 surface molecules were revealed by PE-labeled goat anti-mouse immunoglobulin G (IgG) antibody, and cells were analyzed by flow cytometry.

FACS-based recycling assay. The recycling of HLA-A2 was measured by using an assay adapted from reference (2). HeLa cells were transiently transfected with the indicated HLA-A2 vectors, along with a GFP vector to distinguish the fraction of transfected cells. After 20 h, cells were treated for 2 to 3 h with cycloheximide (100 μg/ml) and removed from the dish with EDTA (2 mM) in PBS. An aliquot of the cells was stained with the BB7.2 MAb, to define HLA-A2 steady-state surface levels. To remove cell-bound β2-microglobulin, the remaining cells were exposed twice for 1 min to an acidic buffer (50 mM glycine, 100 mM NaCl [pH 2.0]). Cells were then washed and resuspended in Dulbecco's modified Eagle's medium containing cycloheximide (100 μg/ml) plus HEPES buffer (pH 7.4) (20 mM). Fetal calf serum was omitted from the medium in order to avoid the presence of exogenous bovine β2-microglobulin. At different periods of time at 37°C, HLA-A2 surface levels were measured by flow cytometry after staining with the BB7.2 MAb. Steady-state surface levels were defined as 100%, and the fluorescence intensity at time zero, after the acidic wash, was defined as 0%.

Cytotoxicity assay. The HLA-A2-restricted CTL clone 161JXA14 recognizes HIV Gag aa 77 to 85 (peptide SL9, SLYNTVATL) (10). CTL assays were performed as described previously (45). Briefly, target cells were labeled with ^{51}Cr for 45 min. After two washes, 10^4 cells (50 μl) were mixed with synthetic peptide (50 μl) at various concentrations and incubated for 45 min at 37°C. Effector cells were then added for 4 h at 37°C, and radioactivity in cell supernatants was counted. The percentage of specific lysis was calculated as [(^{51}Cr release due to peptide − spontaneous release)/(total release − spontaneous release)] × 100. Each experimental data point represents triplicate determinations. For experiments performed with HIV-expressing cells, cells were ^{51}Cr labeled for 45 min 20 h after transfection.

RESULTS

HLA-A2 molecules carrying consensus sorting signals (A2 YSQI or A2 YSQL) are constitutively down-regulated. Our previous experiments demonstrated that Nef-induced MHC-I modulation necessitates tyrosine residue 321, which is located in the cytoplasmic tail of HLA-A and -B heavy chains (21). Since Nef does not phosphorylate this tyrosine, it is likely that other amino acids contribute to the sorting signal revealed by Nef. Tyrosine 321 belongs to a conserved YSQA sequence (Fig. 1A), which almost fits the consensus sorting motif YXXI or YXXL. We therefore asked whether the alanine plays a role in MHC-I stability at the cell surface and susceptibility to Nef.

To determine whether alanine 324 is important for the stability of MHC-I at the cell surface, we constructed HLA-A2 molecules carrying prototypic sorting motifs by exchanging this amino acid for a hydrophobic isoleucine or leucine residue (mutants A2 YSQI and A2 YSQL, respectively), or as a control, for a nonrelated hydrophilic glutamic acid residue (mutant A2 YSQE) (Fig. 1A). A tyrosine 321 mutant (A2 ASQA) highly expressed at the cell surface was also used as a control (21). Surface expression of mutants and parental HLA-A2 carrying the YSQA motif (A2 WT) was measured after transient transfection of expression vectors in HeLa cells, as previously reported (21). Flow cytometry analysis indicated two classes of HLA-A2 mutants with distinct steady-state surface levels (Fig. 1B). A2 WT, A2 ASQA, and A2 YSQE were expressed at similarly high levels (mean fluorescence [MF] of approximately 700 U after staining with the anti-HLA-A2 MAb BB7.2), whereas levels were reduced for A2 YSQI and YSQL (MF of approximately 150 U). These results indicate that the presence of consensus sorting signals in the cytoplasmic tail induces significant down-regulation of MHC-I surface expression.

To investigate whether down-regulation of A2 YSQI and A2 YSQL was due to a misrouting of the molecules, we examined their subcellular localization. HeLa cells, transiently expressing WT or mutant HLA-A2, were analyzed by immunofluores-

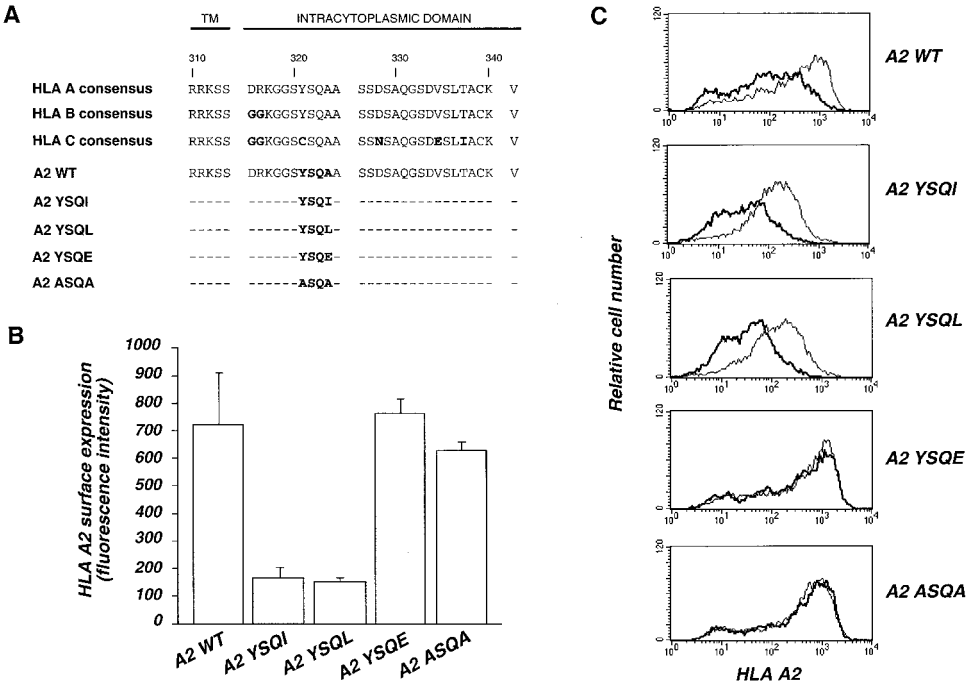

FIG. 1. Surface expression and susceptibility of HLA-A2 mutants to Nef-induced modulation. (A) Amino acid sequence alignment of the cytoplasmic domain of HLA-A, -B, and -C consensus sequences and of A2 WT and point mutants. Dashes represent conserved residues. Consensus sequences and numbering are from reference 29. (B) Surface levels of WT and mutant HLA-A2. HeLa cells were electroporated with 4 μg of the indicated A2 vectors, along with 0.5 μg of a GFP vector. After 24 h, cells were stained with the anti-HLA-A2 MAb BB7.2, and the surface expression of HLA-A2 was measured in GFP-positive cells by flow cytometry. The data are the mean ± standard deviation of three independent experiments. (C) Surface levels of WT and mutant HLA-A2 in the absence or presence of Nef. HeLa cells were electroporated with 12 μg of Nef-FT (bold curves) or Nef-mock (thin curves) vector, along with 4 μg of A2 WT or mutant vectors and 0.5 μg of GFP vector. After 24 h, the surface expression of HLA-A2 was measured in GFP-positive cells by flow cytometry. Data are representative of three experiments.

cence (IF) and confocal microscopy after staining with an anti-HLA-A2 MAb (Fig. 2, left column). As expected, an intense cell surface staining and a weak intracellular signal were detected for A2 WT, A2 YSQE, and A2 ASQA molecules. Surface staining of A2 YSQI or A2 YSQL was strongly reduced, while cytoplasmic dots were visible mostly in the perinuclear region and at the cell margins. Stainings of A2 YSQI or YSQL and clathrin colocalized in the Golgi region and at the cell periphery (not shown). Thus, replacement of alanine 324 of the YSQA motif with glutamic acid did not affect the steady-state surface level nor intracellular localization of MHC-I, whereas creating consensus sorting signals YSQI and YSQL induced constitutive down-regulation and routing towards endocytic compartments. A2 YSQI and YSQL were subsequently referred to as A2-endo.

Effects of Nef and of consensus sorting signals on MHC-I down-regulation. Nef interacts with different components of the cellular trafficking machinery, including the μ chain of AP complexes (21, 32) and β-COP (4, 33). Moreover, in the presence of Nef, MHC-I accumulates in the Golgi region and colocalizes with CCVs (18, 21). To investigate further how Nef facilitates recruitment of MHC-I by the sorting machinery, we performed a comprehensive and comparative analysis of A2-endo- and Nef-induced MHC-I trafficking pathways.

We first examined whether HLA-A2 mutants were susceptible to Nef-induced modulation. WT or mutant HLA-A2 molecules were transiently expressed, with or without Nef, in HeLa cells. Nef expression was verified by Western blotting (not shown). Flow cytometry analysis showed that Nef decreased A2 WT, but not A2 ASQA or A2 YSQE cell surface levels (Fig. 1C). The A2 WT surface level in the presence of Nef was in the range of that observed in cells expressing A2 YSQI or A2 YSQL without Nef (MF of 200 U). Therefore, MHC-I is modulated to a similar extent by Nef and by the presence of a prototypic sorting signal. Interestingly, A2-endo molecules were still susceptible to Nef. A2 YSQI and A2 YSQL surface levels were remarkably low in Nef-expressing cells (MF of 60 U; Fig. 1C). This indicates that Nef and consensus sorting signals exert additional and thus probably distinct effects on MHC-I. Moreover, these data show that Nef-responsive elements within the cytoplasmic tail of MHC-I include the YXXA motif.

We compared the subcellular localizations of HLA-A2 mutants in the absence or in the presence of Nef (Fig. 2). As expected, A2 WT surface staining was reduced in Nef-expressing cells, with bright perinuclear staining and discrete peripheral dots. This cellular distribution of HLA-A2 induced by Nef closely resembles that of the constitutive delocalization of A2-endo molecules (Fig. 2). Nef did not significantly affect the localization of A2-endo, except that A2 YSQI or A2 YSQL

FIG. 2. Subcellular localization of HLA-A2 mutants in the absence or in the presence of Nef. HeLa cells were transfected with 12 μg of Nef-mock (left panels) or Nef-FT (right panels) vector, along with 4 μg of the indicated A2 vectors and a GFP vector. After 24 h, cells were fixed, permeabilized, and stained with an anti-HLA-A2 MAb. The localization of HLA-A2 in GFP-positive cells was examined by immunofluorescence staining and confocal microscopy analysis. Series of optical sections at 0.5 μm were recorded. A representative medial section is shown. Scale bar, 10 μm.

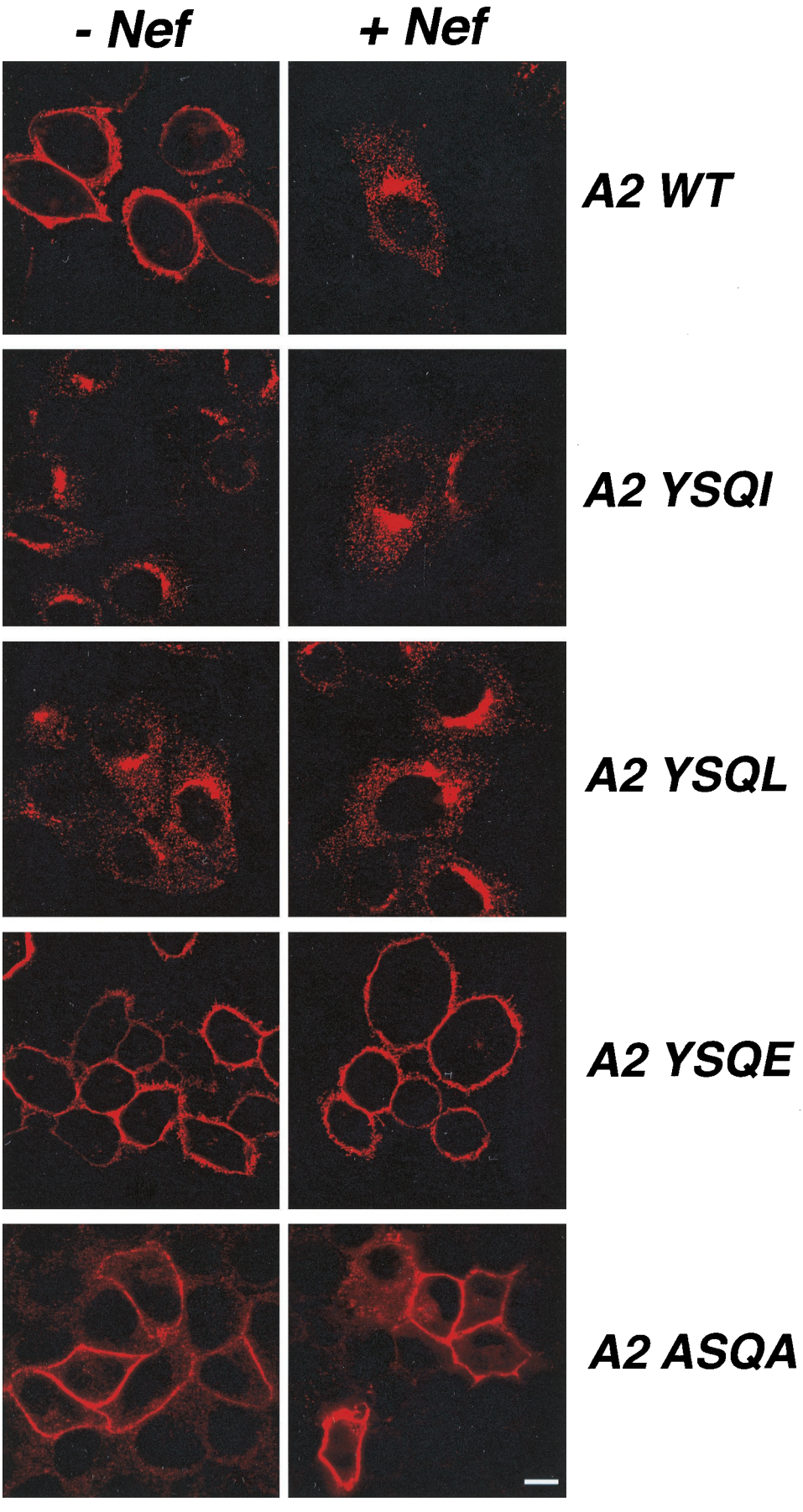
- Nef
+ Nef
A2 WT
A2 YSQI
A2 YSQL
A2 YSQE
A2 ASQA

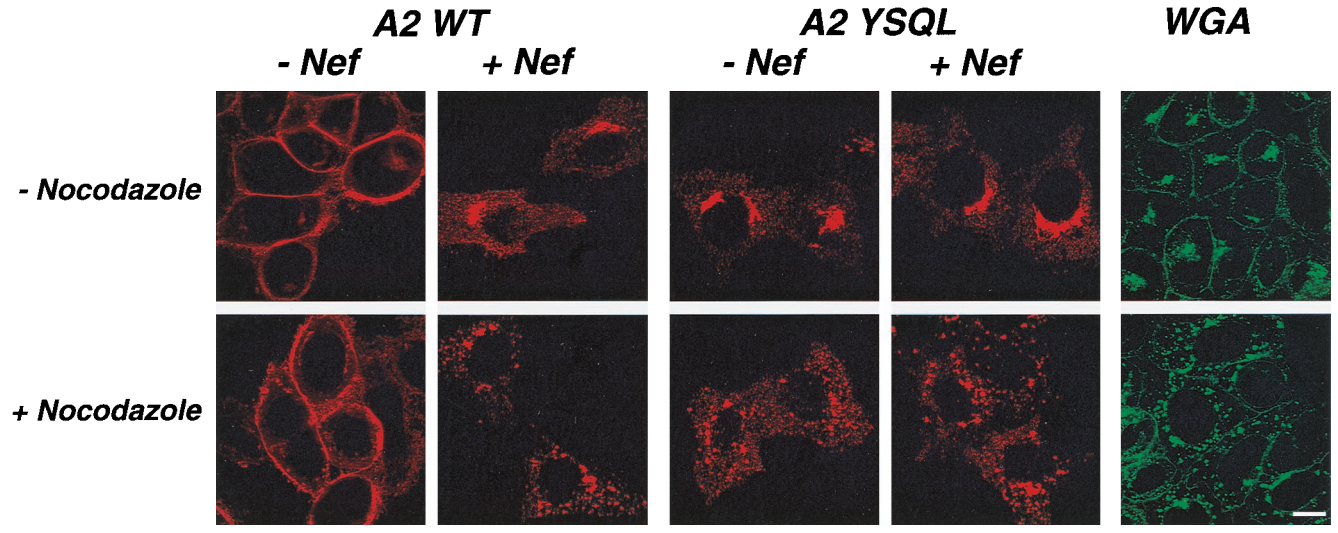

FIG. 3. Susceptibility of A2 WT and A2 YSQL to nocodazole. HeLa cells were transfected with 12 μg of Nef-mock or Nef-FT vector along with 4 μg of A2 WT, or A2 YSQL vector. After 24 h, cells were incubated with (lower panels) or without (upper panels) nocodazole (10 μM) for 1 h before fixation. Localization of HLA-A2 was then analyzed as described in the legend to Fig. 2. To visualize the perturbation of the Golgi network induced by nocodazole, HeLa cells were stained with the Golgi marker WGA conjugated with Alexia 488 (right panels). Scale bar, 10 μm.

perinuclear staining was brighter (Fig. 2). As expected, surface localization of A2 YSQE or A2 ASQA was not affected by Nef (Fig. 2). In Nef-expressing cells, A2 WT, A2 YSQI, and A2 YSQL costained with Golgi markers (rab6 and AP-1) as previously observed for HLA-A2 (21) (not shown).

To further compare the effects of Nef and prototypic sorting signals on MHC-I localization, we used drugs known to perturbate the Golgi network. A2 WT or A2 YSQI molecules were transiently expressed in HeLa cells with or without Nef. One hour prior to HLA-A2 staining, cells were treated with nocodazole or brefeldin A (BFA). Nocodazole depolymerizes microtubules involved in proper localization of the Golgi apparatus, thus leading to breakdown of Golgi structure into large vesicles (15). As expected, A2 WT molecules present at the cell surface were not affected by nocodazole (Fig. 3). In contrast, the constitutive perinuclear staining of A2 YSQL was reduced and replaced by large vesicles (Fig. 3). Similar pictures were observed in Nef-expressing cells for both A2 WT and A2 YSQL (Fig. 3). As a control, cells were stained with the Golgi marker WGA, which selectively binds to sialic acids (*N*-acetylglucosamine and *N*-acetylneuraminic acid) of glycoproteins (49). As expected, nocodazole also induced a redistribution of WGA (Fig. 3).

In the presence of BFA, components of the Golgi apparatus are redistributed to the ER, while the endosomal system tubulates (15). Nef-induced A2 WT, and constitutive A2 YSQL perinuclear stainings were redistributed in BFA-treated cells (not shown). Of note, the effects of nocodazole or BFA were also observed with A2 YSQI (not shown).

These results showed that both Nef and consensus sorting signals down-regulate MHC-I surface expression and induce accumulation in a perinuclear region attached to or juxtaposed with the Golgi. However, the fragmentation pattern of MHC-I induced by nocodazole does not necessarily mean that molecules are located within the Golgi apparatus, since any accumulation of vesicles in the perinuclear region would be similarly disrupted. Nevertheless, one can conclude from susceptibility of staining to nocodazole and BFA that Nef and consensus sorting signals induced accumulation of MHC-I in identical or tightly juxtaposed intracellular compartments.

Analysis of A2-endo- and Nef-induced MHC-I internalization and recycling. (i) Cell surface stability of A2-YSQI or A2-YSQL. Consensus tyrosine-based sorting signals interact with the medium chain (μ) of clathrin-associated AP complexes and are ligands for the sorting machinery at the TGN and the plasma membrane. We examined whether surface A2-endo molecules were rapidly internalized. WT or mutant HLA-A2 molecules were transiently expressed in HeLa cells, and their stability at the cell surface was measured in a flow cytometry-based assay. Staining of surface molecules was performed with the MA2.1 anti-HLA A2 MAb, which does not induce internalization of HLA-A2. Staining of A2 WT, A2 YSQE, and A2 ASQA was high at time zero (MF of 500 U) and remained stable after 30 min at 37°C (Fig. 4A). In sharp contrast, A2-endo molecules displayed low steady-state levels (MF at time zero of 80 and 200 U, for A2 YSQI or A2 YSQL, respectively) and short half-lives at the cell surface (5 to 10 min; Fig. 4A). Therefore, A2-endo molecules are recruited by the sorting machinery, not only in the TGN, but also at the plasma membrane.

(ii) Cell surface stability of HLA-A2 in Nef-expressing cells. We compared the rate of Nef-induced MHC-I endocytosis to those of molecules carrying prototypic sorting signals (Fig. 4B). In Nef-expressing cells, steady-state levels of A2 WT were low (MF at time zero of 200 U), and 70% of molecules remained at the cell surface after 30 min at 37°C. Therefore, although Nef slightly increased the endocytosis rate of A2WT, this effect was limited in comparison with the rapid constitutive internalization of A2 YSQI or YSQL (Fig. 4A). A2 ASQA and A2 YSQE were expressed at high levels at the cell surface and were not internalized in the presence of Nef (not shown). The data are summarized in Fig. 4C, which shows the 5-min time point of the internalization assay. In the absence of Nef, A2 WT was stably expressed at the cell surface, with less than 5% internalization. With Nef, this percentage increased to 25%. Stimulation of endocytosis was much more efficient for A2-endo (40 and 60% internalization for A2 YSQI and YSQL, respectively). The low efficacy of Nef-induced internalization of A2 WT suggests that Nef acts primarily on MHC-I molecules located in the Golgi region.

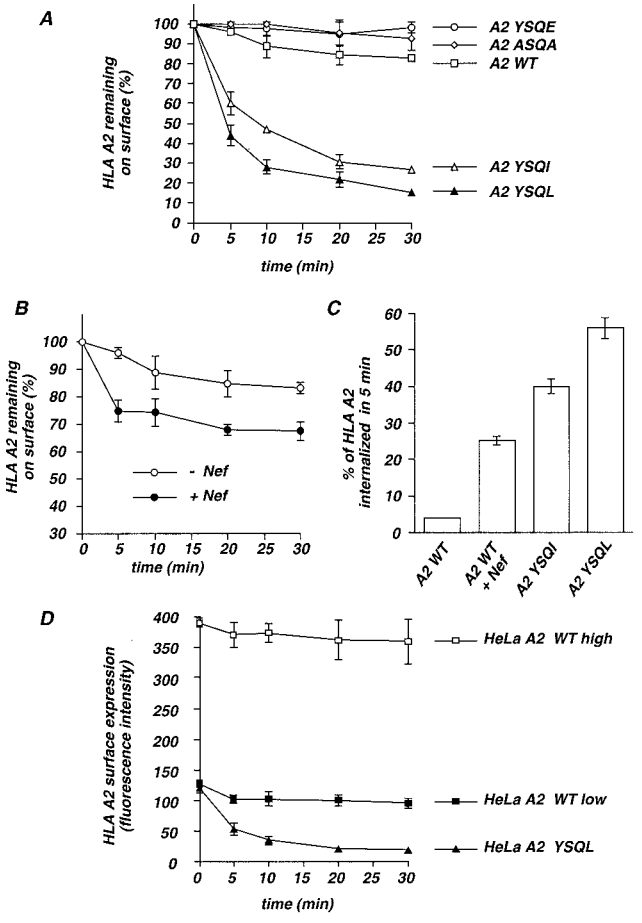

FIG. 4. Effect of prototypic sorting signals and of Nef on the internalization of HLA-A2. (A) Kinetics of internalization of A2 WT and mutants. HeLa cells were transfected with 4 μg of the indicated A2 vectors and 0.5 μg of GFP vector. After 24 h, cells were labeled at 4°C with an anti-HLA-A2 MAb (MA2.1), washed, and incubated at 37°C for the indicated periods of time. Cells were then cooled at 4°C and stained with fluorescent antimouse IgG antibodies. Data are the ratio of the MF at different time points to the value obtained at time zero (400 U for A2 WT, A2 ASQA, or A2 YSQE and 130 U for A2 YSQI and A2 YSQL). Results from three independent experiments (mean ± standard deviation) are shown. (B) Kinetics of internalization of A2 WT in the absence or presence of Nef. HeLa cells were transfected with 4 μg of A2 WT, 12 μg of Nef or Nef-mock vector, and 0.5 μg of GFP vector. Analysis was performed as described for panel A. The surface levels of A2 WT were 400 and 130 fluorescence units, in the absence or presence of Nef, respectively. Results from three independent experiments (mean ± standard deviation) are shown. (C) Comparative analysis of A2 YSQI, A2 YSQL, and Nef-induced HLA-A2 internalization. Internalization rates of HLA-A2 were measured in HeLa cells as described for panels A and B. The 5-min time point is depicted. Results from three independent experiments (mean ± standard deviation) are shown. (D) Kinetics of internalization of HLA-A2 in HeLa clones expressing different steady-state surface levels of A2 WT or A2 YSQL. Independent HeLa clones stably expressing either high (HeLa A2 WT high, 400 U after staining with the MA2.1 anti-HLA A2 MAb) or low (HeLa A2 WT low, 120 U) levels of HLA-A2 WT or expressing A2 YSQL (HeLa A2 YSQL, 120 U) were isolated. Internalization of HLA-A2 was then measured as described above, except that data are presented as the fluorescence intensity of HLA-A2 staining at the indicated time points. For each cell type, results are the mean ± standard deviation of two independent clones.

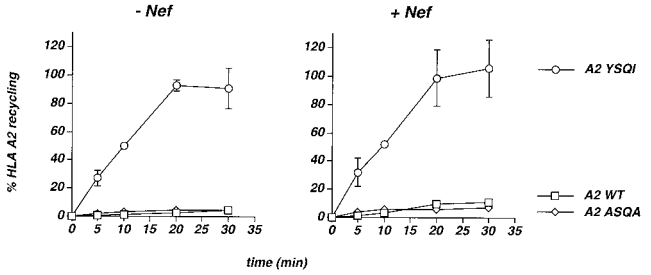

FIG. 5. Effect of prototypic sorting signals and Nef on the recycling of HLA-A2. HeLa cells were transfected with 4 μg of the indicated A2 vectors and 0.5 μg of GFP vector in the absence (left panel) or in the presence of 12 μg of Nef-FT expression vector. After 20 h, cells were pretreated for 2 to 3 h with cycloheximide (100 μg/ml) to eliminate de novo synthesis of MHC-I molecules. An aliquot of the cells was stained with the BB7.2 MAb to define HLA-A2 steady-state surface levels. To disrupt cell surface MHC-I complexes, the remaining cells were exposed to an acidic buffer that removed surface β2-microglobulin. Cells were then incubated at 37°C for the indicated periods of time, and the surface expression of HLA-A2, from a preexisting intracellular pool, was measured by flow cytometry in GFP-positive cells after staining with the BB7.2 MAb. Steady-state surface levels were defined as 100%, and the fluorescence intensity at time zero, after the acidic wash, was defined as 0%. The data show the ratio of the mean fluorescence at different time points to the value obtained for steady-state levels. In a typical experiment, steady-state levels were 750, 690, and 80 U for A2 WT, A2 ASQA, and A2 YSQI without Nef and 210, 680, and 50 U with Nef, respectively. Results from three independent experiments (mean ± standard deviation) are shown.

(iii) Steady-state surface level and internalization rate of HLA-A2 are independent parameters. It was important to rule out the possibility that A2-endo molecules were internalized rapidly because of a low number of molecules at the cell surface. We derived stable HeLa clones expressing either high or low surface levels of A2 WT and compared HLA-A2 internalization rates between these clones. Equivalent stabilities of A2-WT at the cell surface were observed in high (MF of 400 U after staining with the MA2.1 MAb)- or low (MF of 130 U)-expression clones (Fig. 4D). Thus, low surface expression of A2 WT was not associated with rapid internalization rates. In a HeLa clone stably expressing A2 YSQL, the steady-state surface level of A2 YSQL was equivalent to that observed in the HeLa A2 WT low clone (MF of 120 U). However, A2 YSQL was rapidly internalized in this clone, with a half-life at the cell surface of 5 to 10 min (Fig. 4D). Thus, the steady-state surface level and internalization rate of MHC-I are independent parameters.

(iv) Recycling of MHC-I and A2-endo molecules. We investigated the fate of intracellular MHC-I molecules and their ability to reach the cell surface in a FACS-based recycling assay (2). WT or mutant HLA-A2 molecules were transiently expressed in HeLa cells. Surface MHC-I complexes were disrupted by treating cells with an acidic buffer, which removed surface β-microglubulin, resulting in the absence of staining with anti-HLA-A2 MAb BB7.2. Cells were then incubated at 37°C, and the appearance of surface HLA-A2 staining was measured by flow cytometry over time. Steady-state surface staining in the absence of acidic treatment defined 100% levels. Cells were pretreated for 2 to 3 h with cycloheximide (100 μg/ml) in order to suppress de novo protein synthesis. Under these conditions, small amounts of intracellular A2 WT or A2 ASQA gained access to the cell surface (Fig. 5), indicating that these molecules were inefficiently recycled in HeLa cells. In contrast, A2 YSQI staining reached 90% of steady-state levels after 20 min (Fig. 5). Similar results were observed with A2 YSQL (not shown). Thus, A2-endo molecules were constitutively internalized and recycled back to the cell surface. In the presence of Nef, A2 WT and A2 ASQA were still poorly reexpressed at the cell surface, whereas A2 YSQI was still rapidly and efficiently recycled towards the plasma membrane (Fig. 5). Thus, Nef does not affect MHC-I recycling.

Distinct trafficking pathways regulate A2-endo and Nef-induced MHC-I modulation. We investigated the susceptibility of constitutive and Nef-induced down-regulation of mutant

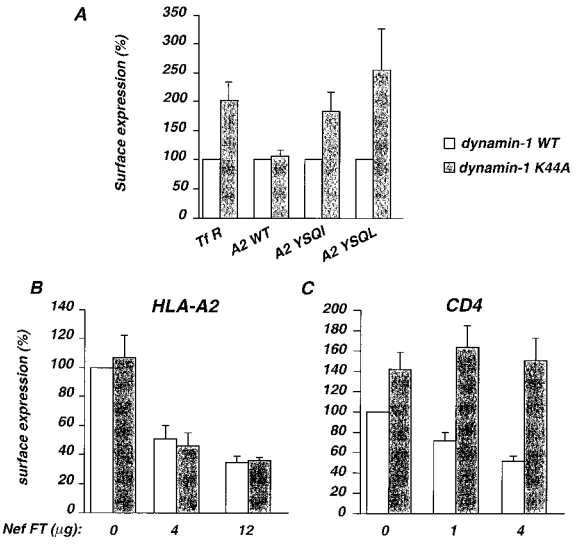

FIG. 6. Susceptibility of A2-endo and Nef-induced HLA-A2 and CD4 modulation to a transdominant-negative dynamin-1 mutant. (A) A2 YSQI and A2 YSQL are endocytosed through a dynamin-1-dependent pathway. HeLa cells were transfected with 4 μg of A2 WT, A2 YSQI, or A2 YSQL vector, along with 30 μg of dynamin-1 WT (white bars) or the transdominant-negative dynamin-1 K44A vector (grey bars), and 0.5 μg of GFP vector. After 24 h, the surface expression of HLA-A2 was measured in GFP-positive cells by flow cytometry. Surface levels of the transferrin receptor (Tf R) were measured as a control for the inhibition of the clathrin-dependent endocytic pathway by dynamin-1 K44A. The data show the steady-state surface levels of the indicated molecules, with 100% corresponding to the levels measured when dynamin-1 WT was expressed. The overexpression of dynamin-1 WT did not affect the surface level of transferrin receptor and of HLA-A2 WT or mutant molecules (not shown). The expression of Nef did not affect that of dynamin-1 WT or mutant proteins, as verified by Western blotting (not shown). (B) Nef-induced MHC-I modulation is not inhibited by dynamin-1 K44A. HeLa cells were transfected with 4 μg of A2 WT, along with either 30 μg of WT (white bars) or K44A dynamin-1 vector (grey bars), and with the indicated amount of Nef vector and 0.5 μg of GFP vector. After 24 h, the surface expression of HLA-A2 was measured in GFP-positive cells by flow cytometry. HLA-A2 steady-state surface levels, measured in the absence of Nef and dynamin-1 K44A, were defined as 100%. (C) Nef-induced CD4 modulation is inhibited by dynamin-1 K44A. HeLa cells were transfected with 2 μg of the CD4 vector of pCCD4, along with either 30 μg of WT (open bars) or K44A dynamin-1 vector (shaded bars), and with the indicated amount of Nef vector and 0.5 μg of GFP vector. After 24 h, the surface expression of CD4 was measured in GFP-positive cells by flow cytometry. CD4 steady-state surface levels, measured in the absence of Nef and dynamin-1 K44A, were defined as 100%. The results from three independent experiments (mean ± standard deviation) are shown.

and WT HLA-A2 molecules to a dominant-negative dynamin-1 mutant. Dynamin-1 is an ~100-kDa protein involved in the formation of clathrin-coated vesicles, which acts in a GTP-dependent manner (41). Dominant-negative dynamin-1 mutant K44A fails to load GTP and blocks formation of clathrin-coated pits and CCVs at the plasma membrane without other obvious effects (12, 41).

We asked whether expression of dynamin-1 K44A interferes with the constitutive endocytosis of A2 YSQL and A2 YSQI. HeLa cells were transiently transfected with A2 WT, A2 YSQI, or A2 YSQL, along with either WT or K44A mutant dynamin-1 expression vectors. Dynamin expression vectors included an HA tag, allowing detection by Western blotting and IF analysis (not shown). As a control for dynamin-1 K44A activity, we showed that its expression induced the expected two-fold increase of transferrin receptor surface levels (12) (Fig. 6A). Dynamin-1 K44A did not significantly affect A2 WT steady-state surface levels (Fig. 6A), thus confirming that MHC-I is stably expressed at the cell surface and not recycled through CCVs in HeLa cells. In contrast, dynamin K44A induced a two- to three-fold increase in A2 YSQI and YSQL steady-state surface levels (Fig. 6A), thus indicating that A2-endo molecules are constitutively endocytosed through an active clathrin-dependent pathway.

We examined whether dynamin-1 K44A inhibits the effect of Nef on MHC-I. HeLa cells were transiently transfected with A2 WT, together with WT or the K44A dynamin-1 vector, and with various amounts of Nef plasmid. HLA-A2 steady-state surface levels measured in the absence of Nef and dynamin-1 K44A were defined as 100% (Fig. 6B). Nef induced MHC-I down-regulation in a dose-dependent manner, with 50 and 30% of HLA-A2 molecules remaining at the cell surface when 4 and 12 μg of Nef plasmid were transfected, respectively (Fig. 6B). Expression of dynamin K44A did not abrogate the down-modulation of HLA-A2 induced by Nef (Fig. 6B). The absence of inhibition persisted when smaller amounts of Nef induced suboptimal modulation of HLA-A2. We conclude that different trafficking pathways are involved in the constitutive internalization of A2-endo and Nef-induced down-regulation of MHC-I.

We also examined the effects of dynamin K44A on Nef-induced CD4 down-regulation. HeLa cells were transiently transfected with a CD4 expression vector, together with WT or K44A dynamin-1 vector, and with various amounts of Nef plasmid. CD4 steady-state surface levels measured in the absence of Nef and dynamin-1 K44A were defined as 100% (Fig. 6C). Nef induced CD4 down-regulation in a dose-dependent manner, with 70 and 50% of CD4 molecules remaining at the cell surface when 1 and 4 μg of Nef plasmid were transfected, respectively (Fig. 6C). The expression of dynamin K44A increased CD4 steady-state surface levels in the absence of Nef. This effect was expected, since CD4 is internalized through clathrin-coated pits in the absence of p56Ick (30). Interestingly, dynamin K44A abrogated the down-modulation of CD4 induced by Nef (Fig. 6C). Thus, Nef acts on MHC-I in a dynamin-1-independent manner and on CD4 in a dynamin-1-dependent manner, indicating that different trafficking pathways mediate Nef-induced MHC-I and CD4 modulation.

Steady-state surface level of MHC-I influences MHC-I-restricted lysis of target cells. We investigated the functional consequences of MHC-I down-regulation, either induced by prototypic sorting signals or by Nef in terms of recognition and killing by specific $CD8^+$ CTLs. We used as an effector the A2-restricted clone 161JXA14 (10), which recognizes a Gag epitope presented by HLA-A2 in HIV-infected cells (45). We first analyzed the influence of steady-state surface levels of MHC-I on the susceptibility of cells to CTLs. HeLa clones expressing various levels of A2 WT were used as targets, following sensitization with the cognate 9-mer peptide SL9. Experiments were performed with two clones expressing high steady-state surface levels of HLA-A2 (HeLa A2 WT high, MF of 1,010 and 900 U, respectively, after staining with the BB7.2 MAb) and with two clones expressing low levels (HeLa A2 WT low, MF of 210 and 260 U, respectively). No lysis was observed when parental HeLa cells, which do not express HLA-A2, were sensitized with the SL9 peptide (not shown). Peptide dose response analysis indicated that HeLa A2 WT high clones were efficiently recognized and lysed by CTLs (Fig. 7A). A maximal lysis of 78% (mean of the two HeLa A2 WT high clones) was observed when cells were preincubated with 1 μg of the peptide per ml. The SD_{50}, which is the peptide concentration giving 50% of maximal specific lysis, was 5 ng/ml. With HeLa A2 WT low clones, maximal lysis was 68% (mean of the two clones) and SD_{50} was 38 ng/ml (Fig. 7A). This experiment indicated that cells expressing three- to fivefold less surface

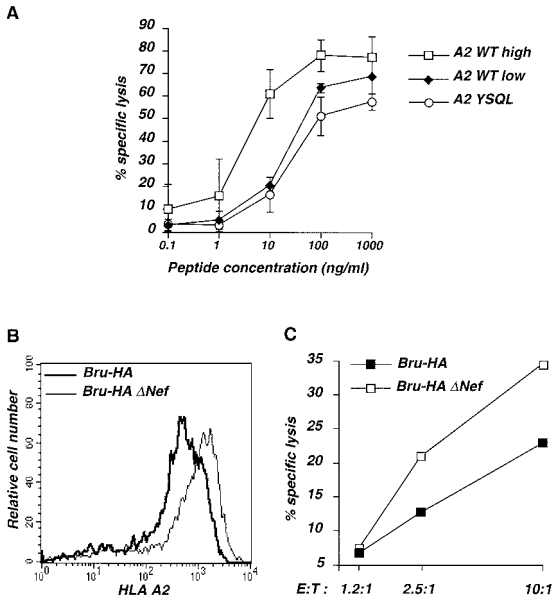

FIG. 7. The HLA-A2 surface level influences lysis of target cells by specific CTLs. (A) Effects of HLA-A2 steady-state level and stability at the surface on CTL-mediated specific lysis of target cells. HeLa cell clones stably expressing high (A2 WT high) or low (A2 WT low) levels of HLA-A2 or expressing A2 YSQL were used as targets in a cytotoxicity assay with the HLA-A2-restricted Gag-specific CTL line 161JXA14. Various concentrations of the cognate Gag peptide (SL9) were added to ^{51}Cr-labeled target cells and remained in the assay during the 4-h incubation of CTLs and target cells. The effector/target cell (E:T) ratio was 5:1. Two independent clones of HeLa A2 WT high (HLA-A2 surface levels of 1,010 and 900 [fluorescent] U after staining with BB7.2, respectively), HeLa A2 WT low (210 and 260 U, respectively), and HeLa A2 YSQL (170 and 270 U, respectively) were analyzed. For each cell type, the data are the mean ± standard deviation percent specific lysis of the two clones. HLA-A2 restriction of the CTL line was confirmed by its inability to kill parental HeLa cells incubated with SL9 or HeLa A2 cells incubated with an irrelevant A2-restricted peptide (not shown). (B) Down-regulation of HLA-A2 in HIV-expressing cells. HeLa cells were grown in six-well plates and transfected with 5 μg of the HIV provirus BRU-HA or BRU-HAΔNef, along with 1 μg of A2 WT vector and 50 ng of GFP vector. After 20 h, the surface expression of HLA-A2 was measured in GFP-positive cells by flow cytometry. The proportions of transfected cells (expressing GFP) were identical for HIV and HIVΔNef and reached 55% (not shown). (C) Nef decreases the killing of HIV-expressing cells by the anti-Gag CTL clone. HeLa cells transiently expressing HIV or HIVΔNef and described for panel B were ^{51}Cr labeled and incubated for 4 h with the HLA-A2-restricted Gag-specific CTL line 161JXA14 at the indicated E:T ratios. Data are the mean of triplicates from one representative experiment. The standard deviation of each experimental point was below 5%. The lysis of HeLa cells transiently transfected with A2 WT only was below 2% (not shown).

HLA-A2 molecules are less susceptible to lysis by the A2-restricted CTL clone and require about eightfold more peptide to reach half-maximum lysis. Therefore, the HLA-A2 steady-state surface level influences the susceptibility of target cells to lysis by CTLs. We then performed similar experiments with two HeLa A2 YSQL clones, in which steady-state surface levels (MF of 170 and 270 U, respectively) were close to those measured in HeLa A2 WT low clones. Maximal lysis was 58% (mean of the two HeLa A2 YSQL clones), and the SD_{50} was 43 ng/ml (Fig. 6A). Therefore, the susceptibility of HeLa A2 YSQL cells to lysis by CTLs was reduced in comparison to that of HeLa A2 WT high, but was not significantly different from that in HeLa A2 WT low.

We then examined the effect of Nef-induced MHC-I modulation on the lysis of HIV-expressing target cells by CTLs. HeLa cells were transiently transfected with the A2 WT vector and with either a Nef-encoding or Nef-deleted HIV molecular clone (HIV or HIVΔnef). Transfections also included a GFP expression vector in order to assess the percentages of transfected cells, which were equivalent with HIV and HIVΔnef and reached 55% (not shown). HLA-A2 surface levels were reduced in cells expressing HIV in comparison with HIVΔnef (Fig. 7B), confirming that the modulation of MHC-I in HIV-infected cells was due to Nef. Levels of Gag protein expression were equivalent with or without Nef, as shown by IF and by Western blot analysis (not illustrated). In the absence of Nef, 35% of the cells were lysed at a 10:1 effector/target ratio (Fig. 7C). Given that only 55% of the cells were transfected and were then true targets for the CTLs, this result indicates that a large majority of target cells were recognized and killed by CTLs. Target cells expressing Nef were less susceptible to killing, with 23% lysed cells (Fig. 7C). These results show that Nef induces the resistance of Gag-expressing cells to CTL killing and are in agreement with a previous report indicating that Nef protects HIV-infected cells against CTLs (10).

Altogether, these experiments indicate that the steady-state surface level of MHC-I, which can be modulated by rapid endocytosis or by the viral protein Nef, influences MHC-I-restricted lysis of target cells.

DISCUSSION

The down-regulation of MHC-I by Nef involves a region of the heavy chain cytoplasmic tail, which is highly conserved in HLA-A and -B. The YSQA sequence located at positions 321 to 324 of HLA-A2 can be considered as a degenerated version of tyrosine-based signals recognized by AP complexes regulating intracellular trafficking, the prototypic sequence of which is YXXI or YXXL. This observation has suggested a model possibly accounting for Nef-mediated down-regulation of MHC-I. According to it, the YSQA motif, which is ignored by the sorting machinery in the absence of Nef, would become recognized by virtue of Nef action. Nef, which physically interacts with μ chains of AP-1 and AP-2, either could make a bridge between μ and MHC-I or could induce modification of μ leading to the recognition of the YSQA motif (21). According to this hypothesis, WT HLA-A2 molecules would exhibit in the presence of Nef a behavior similar to that of mutant HLA-2 molecules displaying prototypic tyrosine-based endocytosis motifs. The aim of the present work was to test this hypothesis. A2-endo molecules, in which the WT YSQA motif was converted to prototypic YSQI or YSQL signals, were constructed with that purpose. Although A2-endo shared several features with those shown by WT HLA-2 in the presence of Nef, evidence exists that distinct mechanisms govern Nef-induced and constitutive AP-mediated endocytosis.

Surface expression of A2-endo was constitutively reduced in comparison with that of WT HLA-A2. The half-life of A2-endo at the surface was shorter than 10 min. Surface levels significantly increased when a transdominant-negative mutant of dynamin-1 (dynamin-1 K44A) was expressed. A2-endo accumulated intracellularly, mostly in perinuclear vesicles, which staining colocalized with that of Golgi markers and clathrin and was affected by drugs modifying the Golgi apparatus. A significant fraction of intracellular A2-endo was rapidly addressed to the cell surface. Taken together, these data indicate that A2-endo molecules were actively internalized through clathrin-coated pits, constitutively routed to the endosomal compartment, and recycled back to the plasma membrane. Thus, down-regulation of A2-endo is likely supported by a direct interaction of prototypic tyrosine-based sorting signals with AP complexes, both at the Golgi and at the plasma membrane. Our results indicate that the spacing of tyrosine-based sorting signals relative to the membrane (40) is adequate for

interaction with the sorting machinery. Thus, the nonrecognition of the WT YSQA motif by the sorting machinery is due to the presence of alanine instead of isoleucine or leucine at residue 324.

In the presence of Nef, WT HLA-A2 exhibited cell surface down-regulation and intracellular accumulation reminiscent of the constitutive modulation of A2-endo. Cell surface molecules were actively internalized. Intracellular staining accumulated in perinuclear vesicles colocalizing with Golgi markers and modified by drugs affecting the structure of the Golgi apparatus. However, our study revealed several distinctive features indicating that molecular mechanisms mediating the action of Nef differ from those responsible for the down-regulation of A2-endo. For equivalent numbers of molecules present at the cell surface, internalization of surface MHC-I induced by Nef was less rapid than that of A2-endo (30 versus 70% internalized molecules after 30 min). MHC-I down-regulation was not affected by a dominant-negative dynamin-1 mutant. WT HLA-A2 molecules accumulating in intracellular vesicles in the presence of Nef were not efficiently addressed to the cell surface. Moreover, A2-endo surface expression was further reduced in the presence of Nef, indicating additional action of Nef on molecules bearing prototypic sorting signals. On the other hand, Nef did not affect the recycling of intracellular A2-endo towards the cell surface. These data indicate a limited effect of Nef on cell surface MHC-I, probably because this action only applies to neo-synthesized MHC-I molecules escaping intracellular retention. Accumulation of newly synthesized molecules in a region assimilable or closely related to the Golgi apparatus appears to be the predominant effect of Nef on MHC-I trafficking. These results render it unlikely that mechanisms supporting the effect of Nef on MHC-I are simple consequences of the disclosure of a cryptic endocytosis signal to the sorting machinery. It is noticeable that neither interaction between Nef and MHC-I, which would support the bridging hypothesis, nor interaction between MHC-I and AP complexes in the presence of Nef, which would support the μ modification hypothesis, has been reported so far.

These conclusions about Nef-induced MHC-I down-modulation contrast with the currently accepted model of Nef-induced CD4 down-modulation. Alteration of CD4 trafficking by Nef involves direct binding of AP complexes to a dileucine-based sorting motif located in the cytoplasmic tail of the molecule. Recognition of this motif by the sorting machinery is presumably responsible for directing cell surface CD4 towards clathrin-dependent endosomal compartments. It is mediated by the interaction of Nef with μ chains, which requires the presence of another dileucine signal in the C-terminal loop of Nef (7, 11, 17, 24). In contrast with CD4, mutation in the dileucine motif of Nef does not affect MHC-I down-regulation (17, 24, 39). Our finding that Nef-induced CD4 but not MHC-I down-regulation is affected by the dynamin-1 K44A transdominant mutant provides additional evidence for distinct mechanisms supporting these effects.

Nef interacts with various components of the cellular trafficking machinery, including β-COP, a component of non-CCVs, and NBP-1, the catalytic subunit of the vacuolar ATPase associated with AP-2 complexes (4, 22). Binding to β-COP or NBP-1 requires diacidic-based motifs located in the C-terminal disordered loop of Nef (EE155 and ED165, respectively) (22, 33). Mutation of these motifs does not affect Nef-induced MHC-I down-regulation (S. Le Gall, unpublished observation), suggesting that β-COP and NBP-1 are not involved in this process. Nef residues associated with the capacity to induce MHC-I down-regulation are located in the N-terminal domain and the polyproline helix of the SH3-binding domain (18, 24). The latter region mediates interactions between Nef and tyrosine or serine and threonine kinases (3). The guanine nucleotide exchange factor Vav also binds to the polyproline motif of Nef, thus activating Vav and subsequent cytoskeletal rearrangements (16). Whether Vav or another SH3-containing protein might be a downstream partner of Nef in MHC-I modulation remains to be determined. Recently, Nef has been reported to bind to the cellular protein PACS-1 (35). PACS-1 was initially described as directing TGN localization of furin by binding to its phosphorylated cytosolic domain (47). Nef interaction with PACS-1 and Nef-induced MHC-I down-regulation are dependent on a cluster of acidic amino acids located in the N-terminal domain of the viral protein. Moreover, MHC-I down-regulation by Nef is partially inhibited in PACS-1 antisense cells. Therefore, Nef may act as a connector between MHC-I and the PACS-1-dependent sorting pathway (35). Our findings that Nef-induced MHC-I down-regulation takes place mostly in the Golgi region and is not affected by a negative transdominant dynamin-1 mutant support this model.

In contrast with HeLa cells and fibroblasts, in which MHC-I is stably expressed at the cell surface, T cells and macrophages exhibit active internalization and recycling of MHC-I in CCVs (23, 25, 38). In B cells, MHC-I molecules are spontaneously internalized and found in endosomes, from which they enter classical MHC-II compartments and are transported back to the plasma membrane (8, 19, 50). Thus, MHC-I molecules lacking so-far-identified prototypic sorting signals can interact with the sorting machinery in the absence of Nef, at least in certain cell types. Mechanisms responsible for cell-type-specific regulation of MHC-I trafficking have not been elucidated. Interestingly, the intensity of Nef-induced MHC-I modulation also varies depending on the cell type. Nef-expressing or HIV-infected HeLa CD4 cells show a threefold decrease in MHC-I steady-state surface levels 21; this study). In contrast, lymphoid cells, such as CEM or Jurkat cells stably or transiently expressing Nef, show a 10-fold decrease in surface MHC-I (18, 42), while a 100-fold decrease has been reported in HIV-infected primary T cells (10). Although part of the observed differences may be attributed to experimental conditions, such as the expressed levels of Nef (21), Nef-induced MHC-I modulation is presumably more efficient in T cells than in other cell types. This observation allows speculation about a possible relationship between constitutive recycling of MHC-I molecules and susceptibility to Nef action.

We have analyzed the functional consequences of MHC-I modulation in terms of recognition and killing by specific CTLs. The epitope density required for a half-maximal cytolytic response by CTLs varies from several thousand peptide-MHC complexes per target cell to fewer than 10, with different combinations of MHC-I, peptides, and CTLs (44). Interestingly, the density of the naturally occurring viral epitope on HIV-infected cells is low compared to the entirety of host cell peptides presented by MHC-I. The abundance of naturally processed HIV peptides was estimated to be in the range of 10 to 400 molecules per infected cell (45). We have shown that a three- to fivefold decrease in the MHC-I steady-state surface level was sufficient to render target cells more resistant to lysis by a specific anti-Gag CTL clone. These results confirm that partial reduction of surface MHC-I in Nef-expressing or HIV-infected cells reduces the efficacy of CTL-mediated cell destruction (10). Thus, Nef might help the virus to evade the CTL response in vivo. HeLa cells expressing A2-endo were more resistant to lysis by specific CTLs than those expressing WT HLA-A2. One can therefore speculate that not only the amount of cell surface HLA antigens, but possibly also the

duration of their presence at the cell surface may be significant in determining the susceptibility to CTL-mediated lysis.

The biological role of endocytosis and recycling of MHC-I has not been fully established. Optimization of peptide loading by MHC-I recycling through early endosomes or classical MHC-II compartments has been reported (1, 8, 19). Endocytosis of MHC-I may also play a role in MHC-I-restricted presentation of exogenous antigens (20, 48). A2-endo molecules provide a valuable tool for studying the various biological aspects of MHC-I post-Golgi trafficking, including internalization and recycling.

ACKNOWLEDGMENTS

We thank E. Perret for confocal microscopy analysis and A. Dautry-Varsat and Y. Rivière for discussions. We thank F. Lemonnier and S. Schmid for the kind gift of reagents.

This work was supported by grants from the Agence Nationale de Recherche sur le SIDA, SIDACTION, and the Pasteur Institute.

REFERENCES

1. **Abdel Motal, U. M., X. Zhou, A. Joki, A. R. Siddiqi, B. R. Srinivasa, K. Stenvall, J. Dahmen, and M. Jondal.** 1993. Major histocompatibility complex class I-binding peptides are recycled to the cell surface after internalization. Eur. J. Immunol. **23:**3224–3229.
2. **Amara, A., S. Le Gall, O. Schwartz, J. Salamero, M. Montes, P. Loetscher, M. Baggioloni, J. L. Virelizier, and F. Arenzana-Seisdedos.** 1997. HIV coreceptor down-regulation as anti-viral principle. SDF-1α dependent internalization of the chemokine receptor CXCR4 contributes to inhibition of HIV replication. J. Exp. Med. **186:**139–146.
3. **Baur, A. S., G. Sass, B. Laffert, D. Willbod, C. Cheng-Mayer, and B. M. Peterlin.** 1997. The N-terminus of Nef from HIV/SIV associates with a protein complex containing Lck and a serine kinase. Immunity **6:**283–291.
4. **Benichou, S., M. Bomsel, M. Bodeus, H. Durand, M. Doute, F. Letourneur, J. Camonis, and R. Benarous.** 1994. Physical interaction of the HIV-1 Nef protein with beta-COP, a component of non-clathrin-coated vesicle for membrane traffic. J. Biol. Chem. **269:**30073–30076.
5. **Bonifacino, J. S., and E. C. Dell'Angelica.** 1999. Molecular bases for the recognition of tyrosine-based sorting signals. J. Cell Biol. **145:**923–926.
6. **Bremnes, T., V. Lauvrak, B. Lindquist, and O. Bakke.** 1998. A region from the medium chain adaptor subunit (μ) recognizes leucine- and tyrosine-based sorting signals. J. Biol. Chem. **273:**8638–8645.
7. **Bresnahan, P. A., W. Yonemoto, S. Ferrel, D. Williams-Herman, R. Geleziunas, and W. C. Greene.** 1998. A dileucine motif in HIV-1 Nef acts as an internalization signal for CD4 downregulation and binds the AP-1 clathrin adaptor. Curr. Biol. **8:**1235–1238.
8. **Chiu, I., D. M. Davis, and J. L. Strominger.** 1999. Trafficking of spontaneously endocytosed MHC proteins. Proc. Natl. Acad. Sci. USA **96:**13944–13949.
9. **Cohen, G. B., R. J. Gandhi, D. M. Davis, O. Mandelboim, B. K. Chen, J. L. Strominger, and D. Baltimore.** 1999. The selective down-regulation of class I major histocompatibility complex proteins by HIV-1 protects HIV-infected cells from NK cells. Immunity **10:**661–671.
10. **Collins, K. L., B. K. Chen, S. A. Kalams, B. D. Walker, and D. Baltimore.** 1998. HIV-1 Nef protein protects infected primary cells against killing by cytotoxic T lymphocytes. Nature **391:**397–401.
11. **Craig, H. M., M. W. Pandori, and J. C. Guatelli.** 1998. Interaction of HIV-1 Nef with the cellular dileucine-based sorting pathway is required for CD4 down-regulation and optimal viral infectivity. Proc. Natl. Acad. Sci. USA **95:**11229–11234.
12. **Damke, H., T. Baba, D. E. Warnock, and S. L. Schmid.** 1994. Induction of a mutant dynamin specifically blocks endocytic coated vesicle formation. J. Cell Biol. **127:**915–934.
13. **Dasgupta, J. D., S. Watkins, H. Slayter, and E. J. Yunis.** 1988. Receptor-like nature of class I HLA: endocytosis via coated pits. J. Immunol. **141:**2577–2580.
14. **Dell'Angelica, E. C., C. Mullins, and J. S. Bonifacino.** 1999. AP-4, a novel protein complex related to clathrin adaptors. J. Biol. Chem. **274:**7278–7285.
15. **Dinter, A., and E. G. Berger.** 1998. Golgi-disturbing agents. Histochem. Cell Biol. **109:**571–590.
16. **Fackler, O. T., W. Luo, M. Geyer, A. S. Alberts, and B. M. Peterlin.** 1999. Activation of Vav by Nef induces cytoskeletal rearrangements and downstream effector functions. Mol. Cell **3:**729–739.
17. **Greenberg, M., L. DeTulleo, I. Rapoport, J. Skowronski, and T. Kirchhausen.** 1998. A dileucine motif in HIV-1 Nef is essential for sorting into clathrin-coated pits and for downregulation of CD4. Curr. Biol. **8:**1239–1242.
18. **Greenberg, M. E., A. J. Iafrate, and J. Skowronski.** 1998. The SH3 domain-binding surface and an acidic motif in HIV-1 Nef regulate trafficking of class I MHC complexes. EMBO J. **17:**2777–2789.
19. **Gromme, M., F. Uytdehaag, H. Janssen, J. Calafat, R. S. van Binnendijk, M. J. H. Kenter, A. Tulp, D. Verwoerd, and J. Neefjes.** 1999. Recycling MHC class I molecules and endosomal peptide loading. Proc. Natl. Acad. Sci. USA **96:**10326–10331.
20. **Jondal, M., R. Schirmbeck, and J. Reimann.** 1996. MHC class I-restricted CTL responses to exogenous antigens. Immunity **5:**295–302.
21. **Le Gall, S., L. Erdtmann, S. Benichou, C. Berlioz-Torrent, L. X. Liu, J. M. Heard, and O. Schwartz.** 1998. Nef interacts with μ subunits of clathrin adaptor complexes and reveals a cryptic sorting signal in MHC-I molecules. Immunity **8:**483–495.
22. **Lu, X., H. Yu, S. H. Liu, F. M. Brodsky, and B. M. Peterlin.** 1998. Interactions between HIV-1 Nef and vacuolar ATPase facilitate the internalization of CD4. Immunity **8:**647–656.
23. **Machy, P., A. Truneh, D. Gennaro, and S. Hoffstein.** 1987. Major histocompatibility complex class I molecules internalized via coated pits in T lymphocytes. Nature **328:**724–726.
24. **Mangasarian, A., V. Piguet, J.-K. Wang, Y.-L. Chen, and D. Trono.** 1999. Nef-induced CD4 and major histocompatibility complex (MHC-I) down-regulation are governed by distinct determinants: N-terminal alpha helix and proline repeat of Nef selectively regulate MHC-I trafficking. J. Virol. **73:**1964–1973.
25. **Neefjes, J. J., V. Stollorz, P. J. Peters, H. J. Geuze, and H. L. Ploegh.** 1990. The biosynthetic pathway of MHC class II but not class I molecules intersects the endocytic route. Cell **61:**171–183.
26. **Ohno, H., J. Stewart, M. C. Fournier, H. Bosshart, I. Rhee, S. Miyakate, T. Saito, A. Gallusser, T. Kirchhausen, and J. S. Bonifacino.** 1995. Interaction of tyrosine-based sorting signals with clathrin-associated proteins. Science **269:**1872–1875.
27. **Oldridge, J., and M. Marsh.** 1998. Nef—an adaptor adaptor? Trends Cell Biol. **8:**302–305.
28. **Owen, D. J., and P. R. Evans.** 1998. A structural explanation for the recognition of tyrosine-based endocytic signals. Science **282:**1327–1332.
29. **Parham, P., E. J. Adams, and K. L. Arnett.** 1995. The origins of HLA-A,B,C polymorphism. Immunol. Rev. **143:**141–180.
30. **Pelchen-Matthews, A., I. Boulet, D. R. Littman, R. Fagard, and M. Marsh.** 1992. The protein tyrosine kinase $p56^{lck}$ inhibits CD4 endocytosis by preventing entry of CD4 into coated pits. J. Cell. Biol. **117:**279–290.
31. **Petit, C., O. Schwartz, and F. Mammano.** 1999. Oligomerization within virions and subcellular localization of human immunodeficiency virus type 1 integrase. J. Virol. **73:**5079–5088.
32. **Piguet, V., Y. L. Chen, A. Mangasarian, M. Foti, J. L. Carpentier, and D. Trono.** 1998. Mechanism of Nef-induced CD4 endocytosis: Nef connects CD4 with the μ chain of adaptor complexes. EMBO J. **17:**2472–2481.
33. **Piguet, V., F. Gu, M. Foti, N. Demaurex, J. Gruenberg, J. Carpentier, and D. Trono.** 1999. Nef-induced CD4 degradation: a diacidic-based motif in Nef functions as a lysosomal targeting signal through the binding of β-COP in endosomes. Cell **97:**63–73.
34. **Piguet, V., O. Schwartz, S. Le Gall, and D. Trono.** 1999. The down-regulation of CD4 and MHC-I by primate lentiviruses: a paradigm for the modulation of cell surface receptors. Immunol. Rev. **168:**51–63.
35. **Piguet, V., L. Wan, C. Borel, A. Mangasarian, N. Demaurex, G. Thomas, and D. Trono.** 2000. HIV-1 Nef protein binds to the cellular protein PACS-1 to downregulate class I major histocompatibility complex. Nat. Cell Biol. **2:**163–167.
36. **Ploegh, H. L.** 1998. Viral strategies of immune evasion. Science **280:**248–253.
37. **Rapoport, I., Y. C. Chen, P. Cupers, S. Shoelson, and T. Kirchhausen.** 1998. Dileucine-based sorting signals bind to the beta chain of AP-1 at a site distinct and regulated differently from the tyrosine-based motif-binding site. EMBO J. **17:**2148–2155.
38. **Reid, P. A., and C. Watts.** 1990. Cycling of cell-surface MHC glycoproteins through primaquine-sensitive intracellular compartments. Nature **346:**655–657.
39. **Riggs, N. L., H. M. Craig, M. W. Pandori, and J. C. Guatelli.** 1999. The dileucine-based sorting motif in HIV-1 Nef is not required for down-regulation of class I MHC. Virology **258:**203–207.
40. **Rohrer, J., A. Schweizer, D. Russell, and S. Kornfeld.** 1996. The targeting of Lamp1 to lysosomes is dependent on the spacing of its cytoplasmic tail tyrosine sorting motif relative to the membrane. J. Cell Biol. **132:**565–576.
41. **Schmid, S. L., M. A. McNiven, and P. De Camilli.** 1998. Dynamin and its partners: a progress report. Curr. Biol. **10:**504–512.
42. **Schwartz, O., V. Maréchal, S. Le Gall, F. Lemonnier, and J. M. Heard.** 1996. Endocytosis of MHC-I molecules is induced by HIV-1 Nef. Nat. Med. **2:**338–342.
43. **Simpson, F., N. A. Bright, M. A. West, L. S. Newman, R. B. Darnell, and M. S. Robinson.** 1996. A novel adaptor-related protein complex. J. Cell Biol. **133:**749–760.
44. **Sykulev, Y., M. Joo, I. Vturina, T. J. Tsomides, and H. N. Eisen.** 1996. Evidence that a single peptide-MHC complex on a target cell can elicit a cytolytic T cell response. Immunity **4:**565–571.
45. **Tsomides, T. J., A. Aldovini, R. P. Johnson, B. D. Walker, R. A. Young, and**

H. N. Eisen. 1994. Naturally processed viral peptides recognized by cytotoxic T lymphocytes on cells chronically infected by human immunodeficiency virus type 1. J. Exp. Med. **180:**1283–1293.
46. **Vega, M. A., and J. L. Strominger.** 1989. Constitutive endocytosis of HLA class I antigens requires a specific portion of the intracytoplasmic tail that shares structural features with other endocytosed molecules. Proc. Natl. Acad. Sci. USA **86:**2688–2692.
47. **Wan, L., S. S. Molloy, L. Thomas, G. Liu, Y. Xiang, S. L. Rybak, and G. Thomas.** 1998. PACS-1 defines a novel gene family of cytosolic sorting proteins required for trans-Golgi network localization. Cell **94:**205–216.
48. **Watts, C.** 1997. Capture and processing of exogenous antigens for presentation on MHC molecules. Annu. Rev. Immunol. **15:**821–850.
49. **Wright, C. S.** 1984. Structural comparison of the two distinct sugar binding sites in wheat germ agglutinin. J. Mol. Biol. **178:**91–104.
50. **York, I. A., and K. L. Rock.** 1996. Antigen processing and presentation by the class I major histocompatibility complex. Annu. Rev. Immunol. **14:**369–396.